



**HAL**  
open science

## Modeling the diversion of primary carbon flux into secondary metabolism under variable nitrate and light/dark conditions

Romain Lariat, Christophe Robin, Cathrine Lillo, Tormod Drengstig, Peter Ruoff

► **To cite this version:**

Romain Lariat, Christophe Robin, Cathrine Lillo, Tormod Drengstig, Peter Ruoff. Modeling the diversion of primary carbon flux into secondary metabolism under variable nitrate and light/dark conditions. *Journal of Theoretical Biology*, 2016, 402, pp.144-157. 10.1016/j.jtbi.2016.05.008 . hal-01477462

**HAL Id: hal-01477462**

**<https://hal.univ-lorraine.fr/hal-01477462>**

Submitted on 23 Aug 2023

**HAL** is a multi-disciplinary open access archive for the deposit and dissemination of scientific research documents, whether they are published or not. The documents may come from teaching and research institutions in France or abroad, or from public or private research centers.

L'archive ouverte pluridisciplinaire **HAL**, est destinée au dépôt et à la diffusion de documents scientifiques de niveau recherche, publiés ou non, émanant des établissements d'enseignement et de recherche français ou étrangers, des laboratoires publics ou privés.

1 Modeling the Diversion of Primary Carbon Flux into  
2 Secondary Metabolism under Variable Nitrate and  
3 Light/Dark Conditions

4 Romain Larbat<sup>a,\*</sup>, Christophe Robin<sup>a</sup>, Cathrine Lillo<sup>b</sup>, Tormod Drenstvig<sup>c</sup>,  
5 Peter Ruoff<sup>b,\*</sup>

6 <sup>a</sup>*INRA UMR 1121 Agronomie & Environnement Nancy-Colmar, TSA 40602, 54518*  
7 *Vandoeuvre Cedex, FRANCE and Université de Lorraine UMR 1121 Agronomie &*  
8 *Environnement Nancy-Colmar, TSA 40602, 54518 Vandoeuvre Cedex, FRANCE*

9 <sup>b</sup>*Centre for Organelle Research, University of Stavanger, Stavanger Innovation Park,*  
10 *Måltidets Hus, 4021 Stavanger, NORWAY*

11 <sup>c</sup>*Department of Computer Science and Electrical Engineering, University of Stavanger,*  
12 *4036 Stavanger, NORWAY*

---

13 **Abstract**

In plants, the partitioning of carbon resources between growth and defense is detrimental for their development. From a metabolic viewpoint, growth is mainly related to primary metabolism including protein, amino acid and lipid synthesis, whereas defense is based notably on the biosynthesis of a myriad of secondary metabolites. Environmental factors, such as nitrate fertilisation, impact the partitioning of carbon resources between growth and defense. Indeed, experimental data showed that a shortage in the nitrate fertilisation resulted in a reduction of the plant growth, whereas some secondary metabolites involved in plant defense, such as phenolic compounds, accumulated. Interestingly, sucrose, a key molecule involved in the transport and partitioning of carbon resources, appeared to be under homeostatic control. Based on the inflow/outflow properties of sucrose homeostatic regulation we propose a global model on how the diversion of the primary carbon flux into the secondary phenolic pathways occurs at low nitrate concentrations. The model can account for the accumulation of starch during the light phase and the sucrose remobilization by starch degradation during the night. Day-length sensing mechanisms for variable light-dark regimes are discussed, showing that growth is proportional to the length of the light phase. The model can describe the complete starch consumption during the night for

---

\*Corresponding authors  
Preprint submitted to *Journal of Theoretical Biology*, April 27, 2016  
Email addresses: [romain.larbat@univ-lorraine.fr](mailto:romain.larbat@univ-lorraine.fr) (Romain Larbat),  
[peter.ruoff@uis.no](mailto:peter.ruoff@uis.no) (Peter Ruoff)

plants adapted to a certain light/dark regime when grown on sufficient nitrate and can account for an increased accumulation of starch observed under nitrate limitation.

14 *Keywords:* sucrose homeostasis, phenolic pathway, starch, negative  
15 feedback, integral control, nitrate availability, day-length measurement

---

## 16 **1. Introduction**

17 Plants live in a world of competition; they need resources (light, nutrients,  
18 water) to grow over neighbors, and need to defend against herbivores and par-  
19 asites. Plant growth relies on processes of cell division, cell elongation and  
20 maintenance within the cell which involve mainly the primary metabolism.  
21 Plant defense, on the other hand, relies notably on the development of dif-  
22 ferentiated structures (such as trichomes, spines) and on the synthesis of  
23 secondary metabolites, such as phenolics, alkaloids, carotenoids and other  
24 products. Plant growth and defense share a common carbon (C) source,  
25 i.e. photosynthates (Loomis (1932); McKey (1974); Bryant et al. (1983)).  
26 The defense costs on plant fitness, the trade-off result between growth and  
27 defense, are of great interest for plant ecologists studying plant-pathogens re-  
28 lationships (Züst et al. (2011); Mooney et al. (2010)). This trade-off between  
29 growth and defense is also an important aspect for agronomists. Under-  
30 standing the relationships between growth and defense will help to develop  
31 new agricultural practices to maintain plant defense while still keeping a high  
32 crop production (ecological intensification concept; for review, see Doré et al.  
33 (2011)).

34  
35 During the last decades, several hypotheses have been suggested to de-  
36 scribe the distribution of resources to growth and defense with respect to  
37 the availability of resources (for review, see Stamp (2003)). Among them,  
38 the Growth Differentiation Balance Hypothesis (GDBH) is considered as the  
39 most mature one (Loomis (1932); Herms and Mattson (1992); Stamp (2004)).  
40 The GDBH states that the growth takes priority over the defense and distin-  
41 guishes three domains of resource availability: (i) a severe resource deficiency  
42 where C assimilation, the relative growth rate and the relative rate of sec-  
43 ondary metabolism are positively correlated to the limiting resource; (ii) a  
44 moderate resource limitation where C assimilation is no longer limited, while  
45 the relative growth rate still is. In this domain, most of the assimilated C

46 that is not used for plant growth is diverted to the secondary metabolism.  
47 It results in a negative correlation between the relative rate of secondary  
48 metabolism and the relative growth rate; (iii) in the third domain, the rel-  
49 ative growth rate is no longer limited and requires the major part of the  
50 assimilated C at the expense of the secondary metabolism whose rate is  
51 maintained at a low level (Herms and Mattson (1992); Le Bot et al. (2009)).

52  
53 Although the GDBH considers any plant resources (except light, which  
54 influences C assimilation more than growth) a large body of the literature  
55 aiming to test this hypothesis has been focused on the nitrate (N) availabil-  
56 ity and led to controversial conclusions. On the one hand, as expected by  
57 the hypothesis, N limited plants generally exhibit a slow growth rate and an  
58 increase in soluble phenolics, a large family of C-rich secondary metabolites  
59 involved in plant defense (Le Bot et al. (2009); Larbat et al. (2012); Royer  
60 et al. (2013); Stewart et al. (2001); Nguyen and Niemeyer (2008); Glynn  
61 et al. (2007)). On the other hand, the content of other C-rich secondary  
62 metabolites like terpenes, tannins and also lignin, the main compound of  
63 the plant structure and cell wall reinforcement, do not follow the predic-  
64 tions of the GDBH (Massad et al. (2012); Koricheva et al. (1998); Royer  
65 et al. (2013)). These examples indicate that global conceptual models could  
66 not properly describe the response diversity of the secondary metabolism to  
67 resources availability. They highlight the need to develop complementary  
68 models taking into account knowledge on key metabolic pools together with  
69 their relationships and regulations. The aim of our present work was to pro-  
70 vide such a model on the impact of N availability on the C flux toward the  
71 primary metabolism and the phenolic pathway taken as representative of the  
72 secondary metabolism.

73  
74 Nitrogen is a major nutrient for plants. It is an essential constituent of  
75 amino acids and proteins, nucleic acids, co-factors and the photosynthetic  
76 apparatus (Chlorophylls, Rubisco), making it a key element to sustain plant  
77 growth (Marschner (2012)). With the exception of legumes, nitrogen is as-  
78 similated by plants through inorganic forms, the major one being nitrate (N)  
79 in aerobic soils (Xu et al. (2012)). N and derived metabolites are also signal-  
80 ing molecules up-regulating genes involved in N assimilation, photosynthesis  
81 and primary metabolism (amino acid synthesis, pentose phosphate path-  
82 way) and repressing the expression of several genes in the phenylpropanoid  
83 pathway (Vidal and Gutierrez (2008); Fritz et al. (2006)). The effect of N

84 limitation on the increase in the phenolic content mentioned above is corre-  
85 lated with an up-regulation of the expression of the phenylpropanoid specific  
86 genes (Fritz et al. (2006); Lillo et al. (2008)). In addition, a limitation in  
87 the N fertilization triggers also a variety of responses in the carbohydrate  
88 and primary metabolisms at the metabolic level that is at least partly due  
89 to large regulations at the transcriptome level (Scheible et al. (2004); Fritz  
90 et al. (2006)). Indeed, the main features observed in plant leaves are a de-  
91 crease in the concentrations of individual amino acids (Fritz et al. (2006)),  
92 proteins (Kingston-Smith et al. (2005)) and organic (citric and malic) acids  
93 (Le Bot et al. (2009); Royer et al. (2013)), an increase in hexoses (Le Bot  
94 et al. (2009)), whereas the concentration of sucrose is maintained nearly con-  
95 stant or is less affected (Le Bot et al. (2009); Fritz et al. (2006); Pretorius  
96 et al. (1999); Abro et al. (2013); Geiger et al. (1999)).

97  
98 Sucrose represents a pivotal molecule for plant metabolism. It constitutes  
99 the major form of C transport between tissues and organs and is also a sig-  
100 naling molecule regulating large aspects of the cell metabolism (for review,  
101 Wind et al. (2010)). During the day, sucrose is synthesized in the cytosol  
102 from the Calvin cycle products (triose phosphates) and, during the night,  
103 from the breakdown of accumulated starch (Stitt and Zeeman (2012); Hu-  
104 ber et al. (1992)). Sucrose biosynthesis is highly regulated notably through  
105 a feed-forward regulation on the fructose-1,6-phosphatase (F1,6Pase) and  
106 a feed-back regulation on the sucrose phosphate synthase (SPS) and the  
107 F1,6Pase (Huber et al. (1992)). The role of sucrose as signaling molecule is  
108 less documented than glucose. However, sucrose was firmly proved, to repress  
109 the expression of plastocyanin, a photosynthetic gene (Dijkwel et al. (1996))  
110 and the transcription factor bZIP11 involved in the regulation of amino acids  
111 biosynthesis in *Arabidopsis* (Hanson et al. (2008)). Sucrose also up-regulates  
112 the expression of anthocyanin genes (Solfanelli et al. (2006)).

113  
114 The conceptual basis of the model we describe in this paper is to consider  
115 the maintenance of the sucrose homeostasis under variable nitrate (N) avail-  
116 ability as a determinant of the C partitionning between the primary and the  
117 secondary metabolisms. When sufficient N is available to the plant, sucrose  
118 is funneled into the primary C metabolism as N activates this pathway (for  
119 review, see Vidal and Gutierrez (2008)). Under these conditions, the sucrose  
120 homeostasis is maintained by an inflow control mechanism (for mechanis-  
121 tic details see next chapter), which provides the sufficient C-flux required

122 by the N activated primary C metabolism. At lower and growth limiting  
123 N conditions, the primary C-flux is diminished due to the lower activation  
124 by N. But, as a consequence of the still unchanged photosynthetic activity,  
125 sucrose is still formed from trioses-P. To keep sucrose at a constant homeo-  
126 static level, the excess of produced sucrose, which cannot enter the primary  
127 C-flux, is now diverted into the secondary C metabolism, by the use of an  
128 outflow mechanism (for mechanistic details see next chapter). The major  
129 metabolic pathway served is thus the soluble phenolics pathway. Besides the  
130 diversion of primary C-flux into the phenolic pathway the model can also  
131 account for the increased accumulation of starch under N limiting condition  
132 and the accumulation and remobilization of starch into sucrose under diurnal  
133 and variable light-dark conditions.

134

## 135 **2. Modeling Sucrose Homeostasis**

136 An essential property of all cells and organisms is their homeostatic regu-  
137 lation of a wide range of components. The term 'homeostasis' was introduced  
138 by Cannon while showing that many compounds and physiological parame-  
139 ters in cells and organisms are kept within certain and often narrow limits  
140 (Cannon (1929)).

141

142 In biochemical systems, robust homeostasis can be achieved by combining  
143 a negative feedback with integral control (Yi et al. (2000)). While robust reg-  
144 ulation by integral control is well established in control engineering (Wilkie  
145 et al. (2002)), kinetic principles leading to integral control in biochemical sys-  
146 tems were only recently found (Ni et al. (2009); Huang et al. (2012); Drengstig  
147 et al. (2012a,b); Thorsen et al. (2013)). These studies showed that homeo-  
148 static controller motifs fall into two classes termed as inflow and outflow  
149 controllers (Drengstig et al. (2012a)). Inflow controllers provide homeostasis  
150 by adding the controlled variable to the system by a compensatory flux from  
151 an internal or external source. Inflow controllers compensate for outflow per-  
152 turbations, which act on the controlled variable. Outflow controllers work  
153 oppositely. They remove the excess of the controlled variable (due to inflow  
154 perturbations) by excreting or moving it to an internal store.

155

156 In the following, we show how the combination of inflow and outflow con-  
157 trollers can describe sucrose homeostasis in plant and the associated daily

158 buildup and degradation of starch at different light-dark regimes. When N  
159 becomes limiting for the plant growth the combined controllers divert the  
160 primary C-flux into the secondary metabolism in order to maintain plant  
161 sucrose homeostasis.

162

### 163 **3. The Model**

164 Fig. 1 gives an overview of the model which is defined at the global plant  
165 scale. Rate equations and parameter values are listed in the appendices  
166 and figure legends, respectively. Sucrose synthesis occurs by two main reac-  
167 tion paths. During the day sucrose is formed by photosynthesis via triose-  
168 phosphates (triose-P). Photosynthetic CO<sub>2</sub> assimilation and regulations are  
169 well described in the literature. For the sake of simplicity these regula-  
170 tions were not considered here. For details, see Farquhar et al. (1980) and  
171 Von Caemmerer and Farquhar (1981). During the night, when there is no  
172 photosynthetic activity, sucrose is formed from starch that has been synthe-  
173 sized during the previous day. At sufficiently high N concentrations sucrose  
174 is directed into the primary C metabolism, which generates compounds in-  
175 volved in plant growth (notably amino acids and proteins). The secondary  
176 C-flux leads to the production of soluble phenolics, which increase in con-  
177 centration when N availability is limiting for the plant growth (Fritz et al.  
178 (2006); Le Bot et al. (2009)). Part of the secondary C-flux leads also to the  
179 synthesis of lignin, but here no regulation has been demonstrated.

180

181 Internal nitrate levels in plant leaves and roots have been found to be un-  
182 der homeostatic control (Miller and Smith (1992, 2008)). In order to account  
183 for this here, the uptake of N is described by an inflow-type of controller as  
184 done previously (Huang et al. (2012)). However, for the sake of simplicity N  
185 storage and remobilization, which take also part in the nitrate homeostatic  
186 mechanism, are not considered here.

187

188 Internal N favors photosynthesis and growth through gene activation (for  
189 review, see Vidal and Gutierrez (2008)). This is represented in the model by  
190 a N-activation of the triose-P formation and the activation of sucrose entry  
191 to the primary C-flux. In the model, the N-activations are described by the

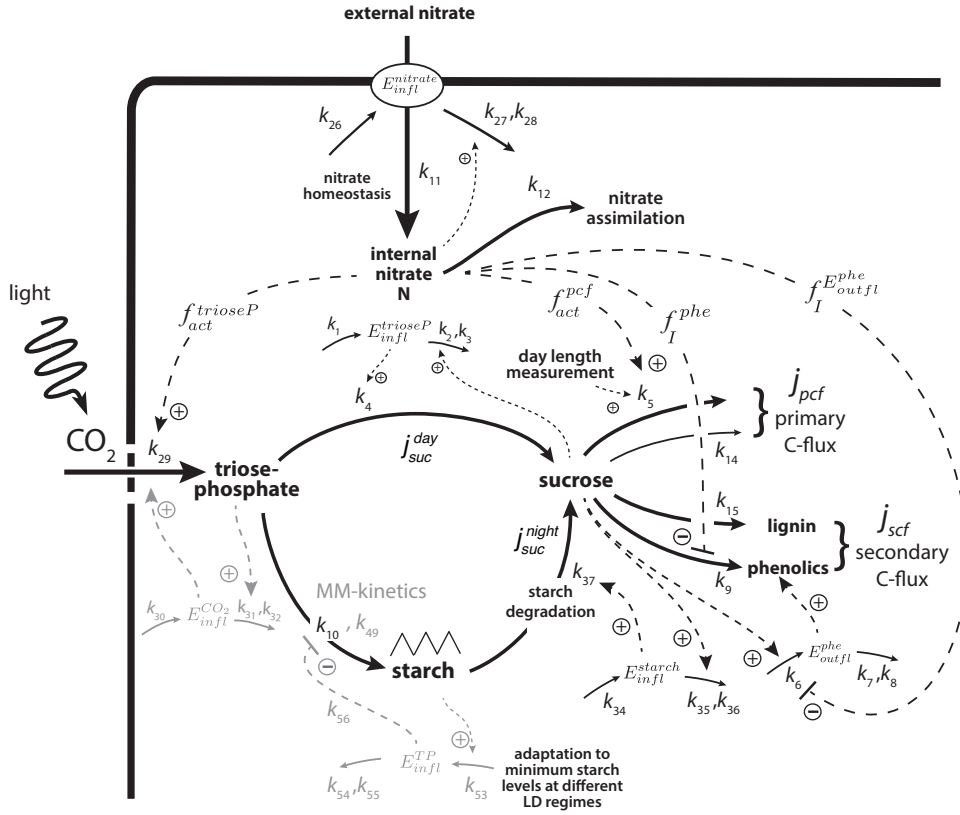


Figure 1: Plant model for sucrose homeostasis under variable nitrate (N) availability. Grayed sections are successively included. During the day, triose-phosphate formed from the photosynthesis is shared between the synthesis of starch and the synthesis of sucrose. Sucrose is used for the formation of primary carbon (C) compounds as well as secondary compounds (phenolics) and lignin. The demand for sucrose is regulated by at least one inflow controller including SnRK1. In the model, this inflow control is represented by  $E_{in\,fl}^{trioseP}$  (see discussion). During the night, sucrose is formed from starch via a remobilization pathway and regulated by inflow controller  $E_{in\,fl}^{starch}$ . The adaptation to a minimal starch level at dawn at different light/dark regimes is performed by a starch inflow controller  $E_{in\,fl}^{TP}$  (outlined in gray). Because internal N is kept at a homeostatic level, maximum activation of the primary C pathway by  $E_{in\,fl}^{trioseP}$  is ensured by sufficient external N concentrations. When external N is getting so low such that the high affinity uptake system of N is not able to maintain internal N homeostasis, the primary C-flux decreases due to a lower N-activation on  $k_5$ . Since photosynthesis is less sensitive to N limitation than growth (due to the different activation constants  $k_{13}$  and  $k_{33}$  in  $f_{act}^{pcf}$  and  $f_{act}^{trioseP}$ , respectively), the N activation on the photosynthetic activity ( $k_{29}$ ) is still maintained and sucrose is still formed. To avoid a build-up of sucrose and to keep sucrose at a homeostatic level, excess of C is diverted by outflow controller  $E_{out\,fl}^{phe}$  into the phenolic pathway (see discussion).



192 activating function

$$f_{act}^X = f_{act,max}^X \left( \frac{N}{K_{act}^X + N} \right) \quad (1)$$

193 where  $N$  is the concentration of nitrate and  $K_{act}^X$  is an activation constant.  
194  $X$  is a variable, which describes the target of the activation, i.e., either  
195 triose-phosphates (triose-P) or the primary C-flux (pcf). When  $N$  is high  
196 compared to  $K_{act}^X$ ,  $f_{act}^X$  reaches its maximum value  $f_{act,max}^X$ . Different  $f_{act,max}^X$   
197 and  $K_{act}^X$  values are assumed for the activation of the primary C metabolism  
198 and triose-P.  $N$  exerts also a repressing effect on the phenolic pathway (Fritz  
199 et al. (2006)), which we have included in the model by inhibitory functions  
200 of the form

$$f_I^Y = f_{I,max}^Y \left( \frac{K_I^Y}{K_I^Y + N} \right) \quad (2)$$

201 where  $Y$  denotes the target compound of the inhibition.

202

203 Remobilization of sucrose from starch is described by an inflow controller  
204  $E_{infl}^{starch}$  with its own homeostatic set-point, considering that the plant has a  
205 demand for sucrose also during the night. To keep sucrose at a robust homeo-  
206 static level, two other control steps are included into the model. When the  
207 demand for sucrose is high at light and high  $N$  concentrations leading to  
208 increased growth rates, the inflow controller  $E_{infl}^{trioseP}$  enables the necessary  
209 sucrose delivery for the primary C metabolism while maintaining sucrose  
210 homeostasis. When  $N$  concentrations become growth-limiting (domain ii of  
211 the GDBH; see above), the primary C-metabolism is reduced, while pho-  
212 tosynthesis is still maintained. Thus, as photosynthesis remains practically  
213 unaltered at growth-limiting conditions, sucrose is still produced and will  
214 eventually exceed the set-point of the inflow controller  $E_{infl}^{trioseP}$ . To avoid a  
215 build-up of sucrose at low  $N$  availability, the excess of produced sucrose is  
216 now redirected into the phenolic pathway by outflow controller  $E_{outfl}^{phe}$ , which  
217 acts concomitantly with the de-repressing effect described by  $f_I^{phe}$ .

218

219 To get a stable production of starch, the triose-P level was kept constant  
220 due to an inflow-type of controller  $E_{infl}^{CO_2}$ . To describe the experimentally ob-  
221 served starch synthesis and degradation at different light-dark regimes molec-  
222 ular mechanisms to measure the amount of received light by the plant are  
223 suggested (see below).

224

225 Rate equations were solved numerically by using the FORTRAN subrou-  
226 tine LSODE (Livermore Solver of Ordinary Differential Equations) (Radhakr-  
227 ishnan and Hindmarsh (1993)) and MATLAB/SIMULINK (www.mathworks.com).  
228 To make notations simpler, concentrations of compounds are indicated by  
229 compound names without square brackets.

230

#### 231 4. Sucrose Homeostasis and Secondary Carbon Flux Induction

232 To illustrate the dynamic behaviors of the model and the diversion of the  
233 primary carbon flux into the phenolic pathway at low external N concentra-  
234 tions, we first consider the situation when different external N concentra-  
235 tions are present. Fig.2 shows a calculation where the external N concentra-  
236 tion successively decreases as N is taken up by the plant. Due to the inflow con-  
237 troller  $E_{in\,fl}^{nitrate}$ , the internal N concentration is kept approximately constant  
238 during its uptake, but decreases rapidly when the external N source becomes  
239 exhausted (Fig 2a). During the uptake of N, the starch content in the cell  
240 increases. During this period, sucrose homeostasis is maintained by inflow  
241 controller  $E_{in\,fl}^{trioseP}$ , while the primary C-flux,  $j_{pcf}$ , is relatively high compared  
242 to the secondary C-flux into the phenolics pathway,  $j_{scf}$  (Figs. 2b and 2c).  
243 For the sake of simplicity the set-point of sucrose was defined to 1. When the  
244 external and internal N concentrations are getting low, there is a phase when  
245 photosynthesis is still operating but the primary C-flux  $j_{pcf}$  is decreasing.  
246 During this stage, starch is still synthesized and sucrose level temporarily  
247 rises (arrow, Fig. 2b). The temporary rise in sucrose level is due to the  
248 decrease in the  $j_{pcf}$  flux by the diminished internal N activation (via  $f_{act}^{pcf}$ ,  
249 Fig. 1) and because the outflow controller  $E_{out\,fl}^{phe}$  has not fully established  
250 its function. Once the outflow controller  $E_{out\,fl}^{phe}$  has taken control, sucrose  
251 is diverted into the phenolic pathway. At this stage, sucrose homeostasis  
252 is re-established and  $j_{scf}$  is at a high level relative to  $j_{pcf}$  (Fig. 2c). When  
253 N availability becomes so low that photosynthesis can no longer be main-  
254 tained, sucrose is synthesized from the starch pool and sucrose homeostasis  
255 maintained by outflow controller  $E_{out\,fl}^{phe}$  until all starch is used up (Fig. 2a).  
256 Fig. 2d shows how  $j_{scf}$  and  $j_{pcf}$  levels from Fig. 2c depend on the amount  
257 of external N and shows their respective up- and down-regulation when ex-  
258 ternal N levels are getting low.

259

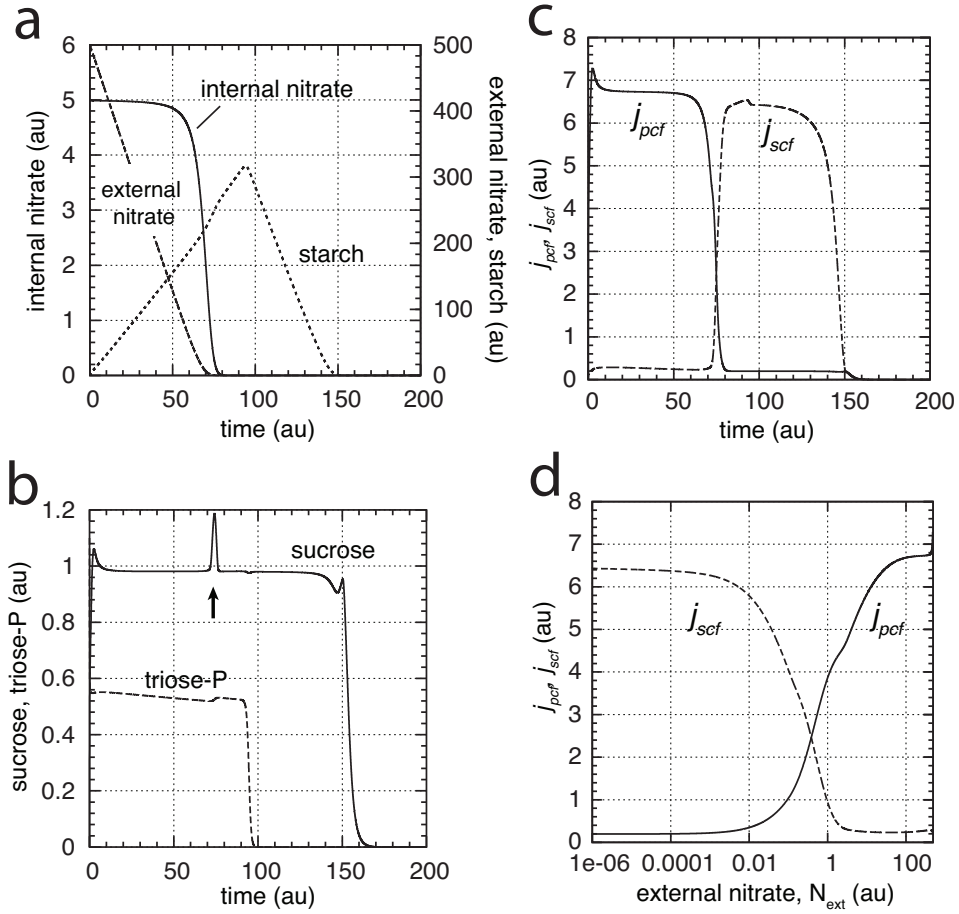


Figure 2: Sucrose homeostasis and the partitioning from the primary C-flux into the secondary metabolism at low external N (without the grayed sections in Fig. 1). (a) Internal N levels are kept under homeostatic control while external N levels are decreasing. During this period, photosynthesis is maintained and triose-P is transformed into starch and sucrose while sucrose levels remain at their homeostatic level. (b) Sucrose homeostasis (with a set-point of 1). (c) Primary and secondary C-fluxes. When external N concentrations become very low, the internal N concentration decreases, which leads to a decrease in the primary C-flux  $j_{pcf}$  and a temporary increase of sucrose (arrow, panel b), but outflow controller  $E_{outfl}^{phe}$  increases  $j_{scf}$  and maintains sucrose homeostasis. (d)  $j_{pcf}$  and  $j_{scf}$  levels at different  $N_{ext}$ . Rate constant values and initial concentrations (in au):  $k_1=1.0$ ,  $k_2=1.0$ ,  $k_3=1.0\times 10^{-5}$ ,  $k_4=1.0$ ,  $k_5=8.0$ ,  $k_6=10.0$ ,  $k_7=9.8$ ,  $k_8=1.0\times 10^{-6}$ ,  $k_9=1.0$ ,  $k_{10}=10.0$ ,  $k_{11}=0.2$ ,  $k_{12}=1.5$ ,  $k_{13}=1.0$ ,  $k_{14}=k_{15}=0.2$ ,  $k_{16} - k_{25}$  not used,  $k_{26}=0.5$ ,  $k_{27}=0.1$ ,  $k_{28}=1.0\times 10^{-6}$ ,  $k_{29}=10.1$ ,  $k_{30}=k_{31}=0.0$ ,  $k_{32}=1.0\times 10^{-5}$ ,  $k_{33}=1.0\times 10^{-11}$ ,  $k_{34}=9.8$ ,  $k_{35}=10.0$ ,  $k_{36}=1.0\times 10^{-4}$ ,  $k_{37}=0.1$ ,  $k_{38}=0.2$ ,  $k_{39}=1.0\times 10^3$ ,  $sucr_0=2.84$ ,  $E_{infl,0}^{trioseP}=8.06$ ,  $E_{outfl,0}^{phe}=1.0\times 10^{-5}$ ,  $N_0=5.00$ ,  $starch_0=0.0$ ,  $N_{ext,0}=500.0$ ,  $E_{infl}^{nitrate}=7.5\times 10^{-2}$ ,  $trioseP_0=1.10$ ,  $E_{infl,0}^{CO_2}=1.0$  (kept constant), and  $E_{infl,0}^{Starch}=1.0\times 10^{-4}$ .

260 We tested the model under high (Fig. 3) and low (Fig. 4) external N  
261 availabilities for three successive nycthemeral periods. In each simulation  
262 the day/night transition was simulated by switching off the constant  $k_{29}$ ,  
263 related to the photosynthesis, which was put back to its initial values at  
264 the end of the night period (Fig 3a). Evolution of triose-P, sucrose, and  
265 the starch pool were followed over the three nycthemeral periods. Triose-P  
266 quickly reached a plateau during the day and then went to zero during the  
267 night, as a consequence of the photosynthesis switch off.

268 Sucrose concentrations show a transient de- or increase after respective light  
269 to dark (L  $\rightarrow$  D) or dark to light (D  $\rightarrow$  L) transitions (Fig 3a), which are  
270 also seen in experiments (see Fig. 4 in Lu et al. (2005)). However, compared  
271 with the experimental results the model transient peaks are relatively large,  
272 which we consider as a model artefact due to the abrupt changes made in  
273  $k_{29}$ .

274 Starch evolution exhibited, as found by experiments (Smith and Stitt  
275 (2007); Gibon et al. (2004)), a typical saw-tooth profile, characterized by a  
276 linear accumulation during the day and an almost complete linear degrada-  
277 tion during the night (Fig. 3c). At high external N availability, the primary  
278 C-flux  $j_{pcf}$  was much higher than the secondary C-flux  $j_{scf}$  (Fig. 3b). Both  
279 fluxes behaved similar to the sucrose evolution, i.e., with an artifactual peak  
280 at the start of light period, then maintaining a steady state level during the  
281 day and the first part of the night, before decreasing at the end of the night  
282 (Fig. 3b). Under limited external N availability, the daily steady state level  
283 of triose-P was increased by about 25% (Fig. 4a). Sucrose was maintained at  
284 its homeostatic set-point as under high N availability, but did not decrease  
285 during the second half of the night (Fig. 4a). The secondary C-flux  $j_{scf}$  was  
286 now clearly higher than  $j_{pcf}$ , although the primary C-flux showed an increas-  
287 ing trend (Fig. 4c). Compared to the high N availability, starch evolution  
288 was characterized by an increased accumulation during the day and a limited  
289 degradation during the night, resulting in starch accumulation day after day  
290 (Fig. 4b). Sucrose-forming fluxes during light ( $j_{suc}^{day}$ ) and dark ( $j_{suc}^{dark}$ ) condi-  
291 tions maintain sucrose homeostasis (Figs. 4a and 4d).

292

## 293 5. Starch Content During Different Light-Dark Regimes

294 Starch accumulation and mobilization is under circadian regulation (Lu  
295 et al. (2005)). The rate of starch degradation is set by mechanisms that

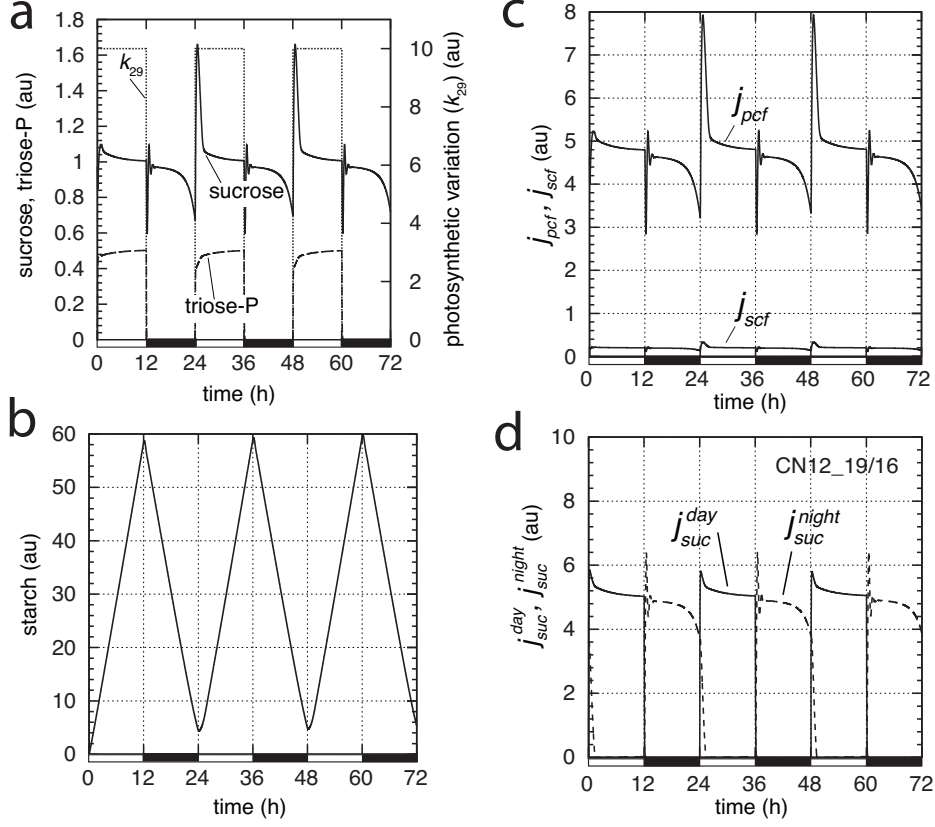


Figure 3: Model calculation at 12h/12h light/dark (LD) changes. At light conditions  $k_{29}=10.1$ , while during darkness  $k_{29}=0.0$ . The concentration of external nitrate ( $N_{ext}$ ) is at a relative high level (20.0) and kept constant. (a) Level of sucrose and triose-P during LD changes. The spikes at the LD transitions are due to the sudden change in  $k_{29}$  and considered as artefacts. (b) At this relative high value of  $N_{ext}$  the primary C-flux,  $j_{pcf}$ , is higher than the secondary one,  $j_{scf}$ . (c) Starch levels show constant synthesis and degradation rates. Rate constant values and initial concentrations (in au):  $k_1=1.0$ ,  $k_2=1.0$ ,  $k_3=1.0 \times 10^{-5}$ ,  $k_4=5.0$ ,  $k_5=5.5$ ,  $k_6=10.0$ ,  $k_7=9.8$ ,  $k_8=1.0 \times 10^{-6}$ ,  $k_9=1.0$ ,  $k_{10}=10.0$ ,  $k_{11}=0.2$ ,  $k_{12}=15.0$ ,  $k_{13}=1.0$ ,  $k_{14}=k_{15}=0.2$ ,  $k_{16} - k_{25}$  not used,  $k_{26}=0.5$ ,  $k_{27}=0.1$ ,  $k_{28}=1.0 \times 10^{-6}$ ,  $k_{29}=10.1$ ,  $k_{30}=k_{31}=0.0$ ,  $k_{32}=1.0 \times 10^{-5}$ ,  $k_{33}=1.0 \times 10^{-11}$ ,  $k_{34}=9.8$ ,  $k_{35}=10.0$ ,  $k_{36}=1.0 \times 10^{-4}$ ,  $k_{37}=0.1$ ,  $k_{38}=2.0 \times 10^{-2}$ ,  $k_{39}=1.0 \times 10^3$ .  $sucr_0=0.748$ ,  $E_{infl,0}^{trioseP}=2.825$ ,  $E_{outfl,0}^{phe}=9.751 \times 10^{-7}$ ,  $N_0=4.998$ ,  $starch_0=6.041$ ,  $N_{ext,0}=20.0$  (kept constant),  $E_{infl,0}^{nitrate}=18.742$ ,  $trioseP_0=0.0$ ,  $E_{infl,0}^{CO_2}=1.0$  (kept constant), and  $E_{infl,0}^{starch}=5.950$ .

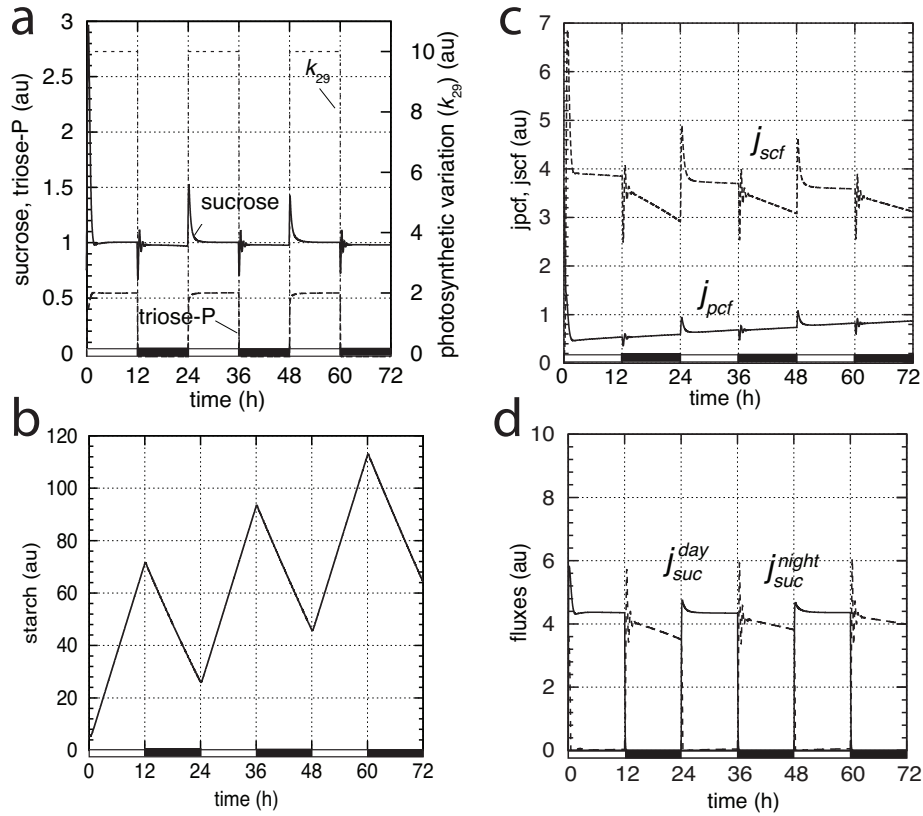


Figure 4: Rate constants and initial concentrations as in Fig. 3, but at low constant  $N_{ext,0}=2.0\times 10^{-2}$ . (a) Sucrose level is kept at its homeostatic set-point of 1.0. (b) As observed experimentally (Le Bot et al. (2009)) starch levels are elevated when external N levels are low. (c) At low  $N_{ext}$  concentrations the  $j_{scf}$  flux is increased to maintain sucrose homeostasis during light and dark conditions. (d) Sucrose forming flux during light ( $j_{suc}^{day}$ ) and dark ( $j_{suc}^{night}$ ) conditions maintaining sucrose homeostasis.

296 'measure' the amount of starch in leaves at the end of the day and anticipate  
297 the length of night in order to maintain a constant supply of C through the  
298 night (Smith and Stitt (2007)). Arabidopsis plants, which are adapted to  
299 different light-dark periods, have been found to regulate their starch con-  
300 tent in such a way that at the end of the night period approximately all  
301 daily produced starch is utilized (Gibon et al. (2004)). The dark circles in  
302 Fig. 5a show the starch content of plants which have been adapted to a 6:18  
303 light:dark regime, while the open squares show the starch content in plants  
304 adapted to a 12:12 light:dark regime. How plants manage to optimize their  
305 starch usage under different light dark conditions is still not well understood  
306 and different approaches have been suggested (Feugier and Satake (2013);  
307 Scialdone et al. (2013); Pokhilko et al. (2014); Seaton et al. (2014); Pokhilko  
308 and Ebenhöh (2015); Scialdone and Howard (2015)). In the following we give  
309 a brief description of these approaches.

310

311 In the work by Feugier and Satake (2013) the optimization of starch us-  
312 age is accomplished by a feedback relationship between the circadian clock  
313 affecting the sucrose/starch metabolism which feeds back to the clock and  
314 induces phase shifts. Their modeling results show that almost all features of  
315 experimental starch profiles can be explained by their feedback hypothesis.  
316 Scialdone et al. (2013) and Scialdone and Howard (2015) suggested a mech-  
317 anism which can be associated with a arithmetic division calculation that  
318 anticipates dawn. They introduce a set of models where the starch degra-  
319 dation rate is determined by the concentration of T-molecules, which reflect  
320 the remaining amount of time ( $\Delta t$ ) until the next dawn, together with the  
321 concentration of S-molecules, which reflect the total starch content. Their  
322 model assumptions lead to the starch degradation rate

$$r = f \cdot \frac{\Delta S^{tot}}{\Delta t} \quad (3)$$

323 The factor  $f$  depends on several structural parameters and kinetic constants.  
324 In order to get a complete starch consumption by the time of expected dawn  
325  $f$  needs to meet the requirement  $f=1$ . The work by Seaton et al. (2014) used  
326 three models to explain the control of starch turnover by the circadian clock.  
327 All three models involve different interlocked feedback loops, but lead to sim-  
328 ilar results. The authors conclude that additional experiments are needed to  
329 elucidate pathway structure together with an identification of the involved  
330 molecular compounds. Seaton et al. (2014) further show how their models

331 provide simple biochemical realizations of the arithmetic division calculation  
332 that have been proposed by Scialdone et al. (2013). The modeling approach  
333 by Pokhilko et al. (2014) and Pokhilko and Ebenhöf (2015) focus on the  
334 regulation of the carbon metabolism using a circadian timer. The regula-  
335 tion of the C-status is mediated by the kinase SnRK1, while the timing is  
336 achieved by the osmotic sensitive kinase OsmK via a circadian regulation of  
337 a  $\text{Ca}^{2+}$ -dependent kinase. Interestingly, in our homeostatic approach the C-  
338 status sensing kinase SnRK1 is related to the inflow homeostatic regulation  
339 of sucrose (see below).

340

341 When testing our model for the behavior shown in Fig. 5a by using dif-  
342 ferent day lengths  $\Phi_L$ , a linear relationship between  $k_5$  and  $\Phi_L$  is found  
343 (Fig. 5b). This relationship predicts that the primary carbon flux increases  
344 proportionally with the day length. This fits very well with many observa-  
345 tions that plant growth is generally proportional to the length of the daily  
346 exposure to light in the absence of other limiting factors (Garner and Allard  
347 (1920); Romberger (1963)). Fig. 5c shows the model's starch synthesis and  
348 degradation behavior for different but constant day lengths. In good agree-  
349 ment with experimental results (Eimert et al. (1995); Gibon et al. (2004);  
350 Lu et al. (2005); Zhang et al. (2005), the model shows that for  $\Phi_L < 12\text{h}$   
351 the rate of starch synthesis is higher during the shorter light period than the  
352 rate of starch degradation during the longer dark period. For  $\Phi_L > 12\text{h}$  the  
353 reverse is observed, i.e., the rate of starch synthesis is now lower during the  
354 longer light period than the rate of starch degradation during the shorter  
355 dark period. When  $\Phi_L = 12\text{h}$  the rates of starch synthesis and degradation  
356 are approximately equal.

357

358 Thus, the model predicts that the ability of the plant to measure the  
359 amount of received light, i.e., the day length, is crucial for the regulation  
360 of its starch utilization. How organisms get information about day length  
361 and use it for physiological purposes such as flowering or growth has been a  
362 long-standing topic within circadian rhythm research (Bünning (1973); Taiz  
363 et al. (2015)).

364

365 We have investigated two hypothetical mechanisms for sensing the day  
366 length with respect to primary carbon metabolism/growth. The first one is  
367 based on two compounds M1 and M2, where M1 is synthesized/activated by  
368 light and is a precursor of M2. The conversion from M1 to M2 is suppressed



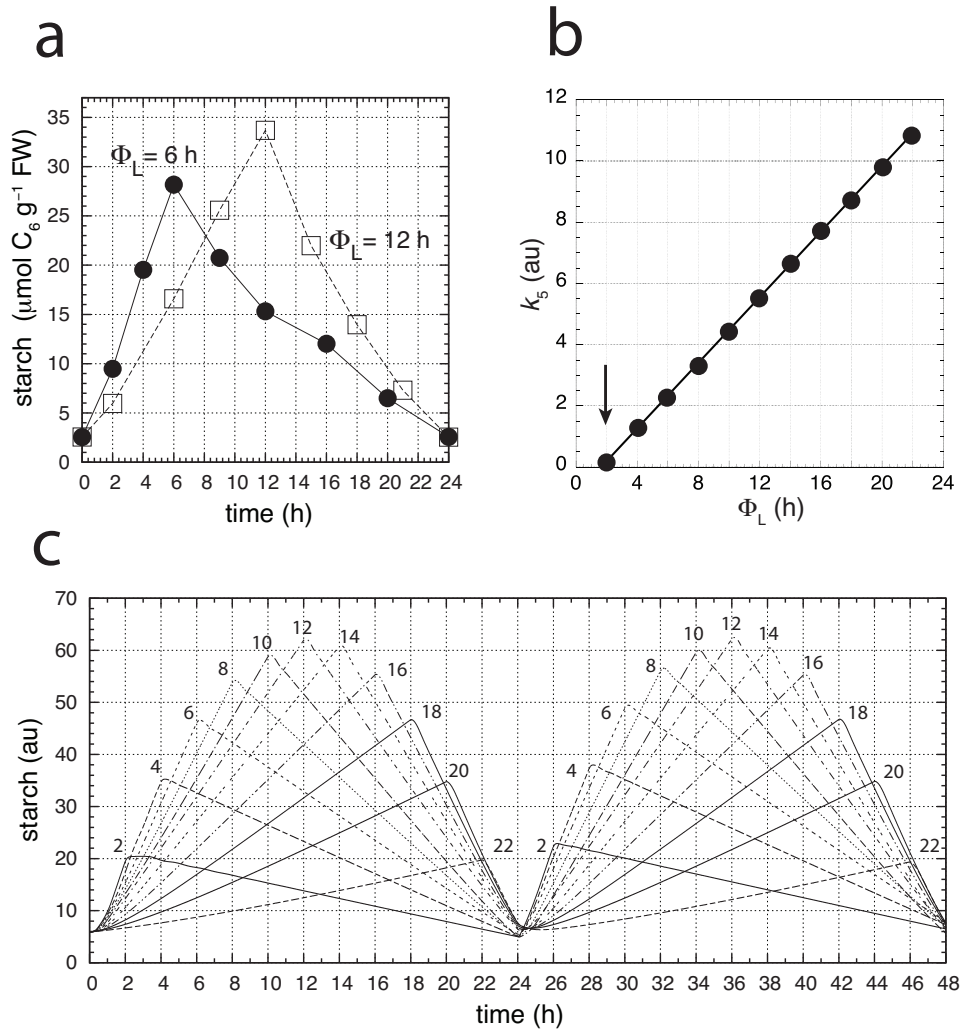


Figure 5: Starch regulation at different light-dark (LD) cycles. (a) Starch levels in Arabidopsis plants adapted to 6h/18h and 12h/12h L/D cycles.  $\Phi_L$  describes the day length. In the LD adapted plants, the production of starch during the day matches precisely its consumption during the following night (Gibon et al. (2004)). (b) In order to achieve that the amount of produced starch during the day matches the amount of starch consumed during the next night, the model predicts that  $k_5$ , i.e., part of the primary C-flux, needs to be proportional to the day length  $\Phi_L$ . The arrow indicates the plant's compensation point, i.e., a minimum day length is required to maintain the system even when no starch is produced. (c) Behavior of starch levels at different day lengths  $\Phi_L$  when  $k_5$  follows the relationship in panel b. The other rate constants and initial concentrations are as in Fig. 3.

369 by light and occurs only in darkness, while the deactivation of M2 occurs  
 370 also in light and at the same rate as M1 is formed. Fig. 6b shows that the  
 371 sum of M1 and M2 is directly proportional to the length of the light phase  
 372  $\Phi_L$ . Both M1 and M2 activate the primary C-flux by the relationship

$$k_5 = \alpha(M1 + M2) - \beta \quad (4)$$

373 The parameter  $\alpha$  is a scaling factor, while  $\beta$  is related to the light compensa-  
 374 tion point, i.e., accounting for that a certain amount of the light/photosynthesis  
 375 is required to maintain respiration at zero growth at which (arrow in Fig. 5b).  
 376 The level of M2 is constant during darkness and reflects the total amount of  
 377 light received during the previous light period. Fig.6c shows the levels of M1,  
 378 M2, and their sum when the light dark regime is changed (see arrow) from  
 379 8h:16h light:dark cycles (short day, SD) to 16h:8h (long day, LD) occurring  
 380 at time  $t=48h$ . M1 increases during the light phase and is converted to M2  
 381 in the beginning of the night. During the night M1 is zero, while M2 stays  
 382 at the maximum level of M1, which has built up during the preceding day.  
 383 At the beginning of the day M1 increases again while M2 decreases.

384

385 Another mechanism, based on the homeostatic behavior of a negative  
 386 feedback loop is shown in Fig. 6d. Here, compound M is generated by  
 387 light where M induces its own repressor E, which inactivates/removes M.  
 388 For low  $K_M^E$  values, M is under a robust homeostatic control (Drengstig  
 389 et al. (2012a)). Under such conditions the steady state level of E reflects  
 390 the amount of light received, i.e., it is proportional to the day length  $\Phi_L$   
 391 (Fig. 6e). In Fig. 6f we show how the day length sensing mechanism works  
 392 when going from short days ( $\Phi_L=8h$ ) to long days ( $\Phi_L=16h$ ). The system  
 393 needs a certain adaptation time until homeostasis in the average level of M  
 394 is achieved. The corresponding value of E is a measure for the day length.  
 395 The time needed for M to reach its set-point is dependent on the magni-  
 396 tudes of the rate constants  $k_{52}$  and  $k_{53}$ , which also determine the set-point  
 397 value  $M_{set}$ .  $M_{set}$  can be found by setting the rate equation of E to zero, i.e.,  
 398  $M_{set}=k_{53}/k_{52} \cdot (E/(K_M^E+E)) \approx k_{53}/k_{52}$ , when  $K_M^E \ll E$ . The adaptation time  
 399 of the controller can be varied by in- or decreasing  $k_{52}$  and  $k_{53}$  while keep-  
 400 ing their ratio constant. This generally will lead to a de- or increase in the  
 401 adaptation time while  $M_{set}$  remains unchanged.

402

403 An interesting observation (Lu et al. (2005)) is that during the first night  
 404 after the transition from a short day (SD) to a long day (LD), the starch

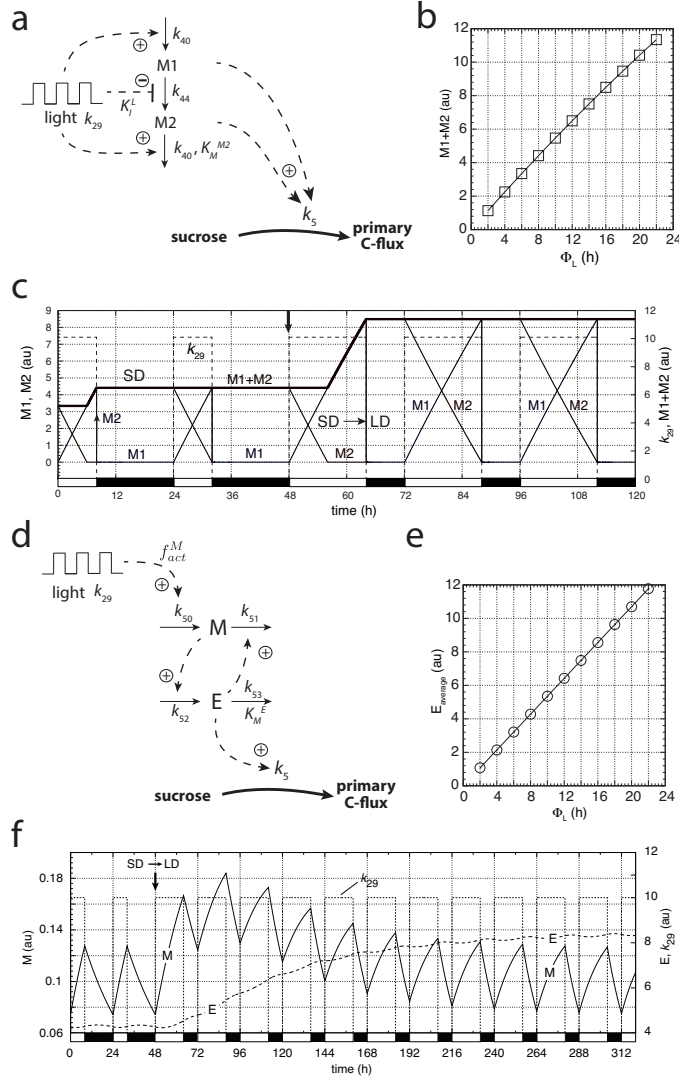


Figure 6: Two hypothetical mechanisms to measure day length. Rate equations are given in the Appendix. (a) Mechanism based on light-activation of M1 and its transfer to M2 during the night. (b) The sum of M1 and M2 are proportional to the day length. Rate constants:  $k_{40}=0.05686$ ,  $k_{44}=1.0 \times 10^3$ ,  $K_I^L=1.0 \times 10^{-4}$ ,  $K_M^{M2}=1.0 \times 10^{-6}$ . Initial concentrations for M1 and M2 are zero. (c) Time profile of M1 and M2 when L/D cycles are changed from 6h/18h to 18h/6h, respectively.  $M1_0=0.0$ ,  $M2_0=3.34$ . (d) Mechanism for day length measurement based on robust homeostasis of light-induced species M. (e) In the mechanism from panel d the average value of controller E is proportional to the day length  $\Phi_L$ . Rate constant values:  $k_{29}=10.0$  (light phase) or 0.0 (dark phase),  $K_a^L=990$ ,  $k_{51}=0.00779$ ,  $k_{52}=0.7$ ,  $k_{53}=0.07$ ,  $K_M^E=1.0 \times 10^{-4}$ . (f) Transition from short day (SD,  $\Phi_L=8.0h$ ) to long day (LD,  $\Phi_L=16.0h$ ) conditions at  $t=48h$  (indicated by arrow).  $M_0=0.075$ ,  $E_0=4.277$ .

405 degradation rate is already increased (Fig. 7a). We have tested the model in  
406 this respect, which clearly shows this behavior (Fig. 7b). However, in order  
407 to keep the starch content at the end of the dark period adapted to low levels  
408 an additional negative feedback together with Michaelis-Menten kinetics is  
409 introduced, which in Fig. 1 is outlined in grey. Fig. 7c shows the LD starch  
410 adaptation when going from SD ( $\Phi_L=8h$ ) to LD ( $\Phi_L=16h$ ). The curve from  
411 48h to 72 is identical to the one dotted in Fig. 7b.

412

## 413 6. Discussion

414 The main features of the model are based on the observations that su-  
415 crose serves as a hub between primary and secondary metabolite pathways  
416 (Wind et al. (2010)), that N activates and inhibits primary and secondary  
417 metabolism, respectively, and that sucrose levels are under homeostatic con-  
418 trol. Sucrose is the major transport form of carbohydrates in higher plants  
419 and is also the major osmotic compound in the phloem sap. The appar-  
420 ent constancy of sucrose levels in the phloem sap were first demonstrated  
421 by Milburn and coworkers when investigating variable sucrose and potas-  
422 sium exudation rates along with the respective concentrations and fluxes for  
423 sucrose and potassium (Smith and Milburn (1980)). By using NMR spec-  
424 troscopy, the study by Peuke et al. (2001) indicated a diurnal variation of  
425 sucrose in 35-45 days old *Ricinus* plants with an approximately 25% increase  
426 in sucrose concentration during the light period. Recently, Kallarackal et al.  
427 (2012) reviewed the literature on sucrose homeostasis and by quantifying  
428 sap sucrose levels using an enzymatic technique concluded that the sucrose  
429 concentrations in young *Ricinus* plants showed only a marginal diurnal vari-  
430 ation. Le Bot et al. (2009) determined the concentrations for several primary  
431 and secondary compounds in leaves of young tomato plants as a function of  
432 external N concentration, including various sugars and sucrose. The studies  
433 by Le Bot et al. showed clearly the up-regulation of secondary metabolites  
434 at low N availabilities, while average sucrose levels remained unchanged. Al-  
435 though diurnal variations in sucrose levels cannot be excluded, these studies  
436 strongly indicate that sucrose is under a homeostatic regulation.

437

438 Homeostasis (Cannon (1929)) involves a combined set of controller motifs,  
439 which adjust the inflow and outflow fluxes of the controlled variable in such  
440 a way that the concentration of the controlled variable is kept within tolera-

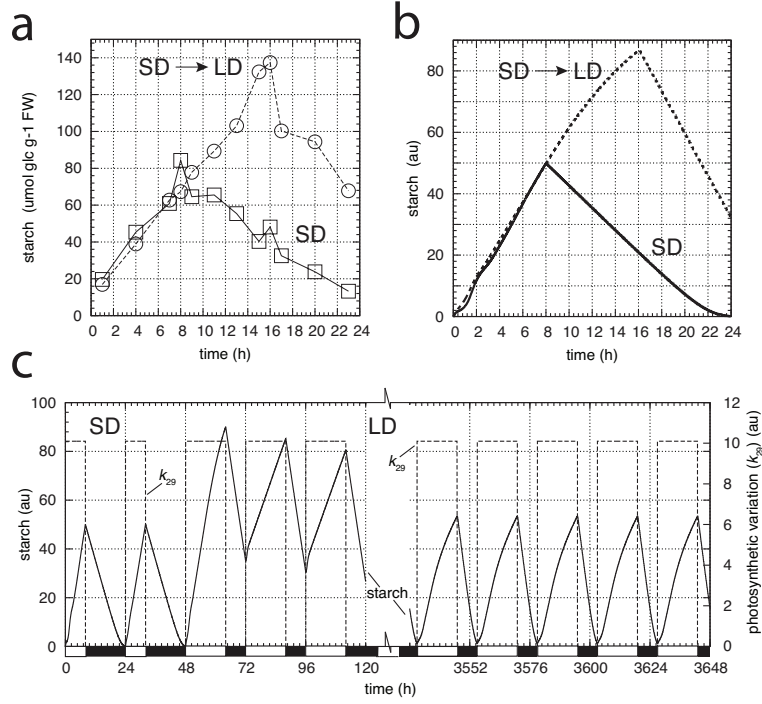


Figure 7: Starch transition kinetics from short days (SD) to long days (LD). (a) Experimental starch profiles of SD adapted Arabidopsis plants directly after the SLDL transition (Lu et al. (2005)). Panel b shows the overlay of the calculated starch profiles (see also panel c) between SD-adapted plants (24h-48h) and the first cycle at LD-conditions (48h-72h). (c) Adaptation behavior in starch profile when going from short days ( $\Phi_L=8.0\text{h}$ ) to long days ( $\Phi_L=16.0\text{h}$ ) at  $t=48\text{h}$ . The mechanism shown in Fig. 6a is used to measure day length  $\Phi_L$ . To describe the behavior predicted in Fig. 5b,  $k_5$  is calculated according to the relationship:  $k_5=M1+M2-0.85$ . To achieve a stable average starch concentration at different LD phases, the gray outlined parts in Fig. 1 are included using  $E_{infl}^{TP}$  as an inflow controller with respect to starch. The set-point of this controller is determined by the condition  $dE_{infl}^{TP}/dt=0$ , which is given by  $(k_{54}/k_{53}) \cdot E_{infl}^{TP} / (k_{55} + E_{infl}^{TP}) \approx (k_{54}/k_{53})$ . Rate constant values and initial concentrations:  $k_1=1.0$ ,  $k_2=1.0$ ,  $k_3=1.0 \times 10^{-5}$ ,  $k_4=5.0$ ,  $k_6=10.0$ ,  $k_7=9.8$ ,  $k_8=1.0 \times 10^{-6}$ ,  $k_9=1.0$ ,  $k_{10}=10.0$ ,  $k_{11}=0.2$ ,  $k_{12}=15.0$ ,  $k_{13}=1.0$ ,  $k_{14}=k_{15}=0.2$ ,  $k_{26}=0.5$ ,  $k_{27}=0.1$ ,  $k_{28}=1.0 \times 10^{-6}$ ,  $k_{29}=10.1$ ,  $k_{30}=0.1$ ,  $k_{31}=2.0$ ,  $k_{32}=1.0 \times 10^{-6}$ ,  $k_{33}=1.0 \times 10^{-11}$ ,  $k_{34}=9.8$ ,  $k_{35}=10.0$ ,  $k_{36}=1.0 \times 10^{-4}$ ,  $k_{37}=0.1$ ,  $k_{38}=2.0 \times 10^{-2}$ ,  $k_{39}=1.0 \times 10^3$ ,  $k_{40}=5.68 \times 10^{-2}$ ,  $k_{44}=1.0 \times 10^3$ ,  $K_I^L=1.0 \times 10^{-4}$ ,  $K_M^{M2}=1.0 \times 10^{-6}$ ,  $k_{49}=1.0 \times 10^{-3}$ ,  $k_{53}=2.5 \times 10^{-4}$ ,  $k_{54}=6.25 \times 10^{-3}$ ,  $k_{55}=1.0 \times 10^{-4}$ .  $\text{sucr}_0=5.140 \times 10^{-5}$ ,  $E_{infl}^{\text{trioseP}}=6.012$ ,  $E_{outfl}^{\text{phe}}=38.677$ ,  $N_0=5.0$ ,  $\text{starch}_0=1.046 \times 10^{-7}$ ,  $N_{ext,0}=20.0$  (kept constant),  $E_{infl}^{\text{nitrate}}=18.75$ ,  $\text{trioseP}_0=0.0$ ,  $E_{infl}^{CO_2}=2.773$ ,  $E_{infl}^{\text{starch}}=55.574$ ,  $M1_0=0.0$ ,  $M2_0=3.342$ , and  $E_{infl}^{TP}=0.0$ .

441 ble limits for the cell/organism (Drengstig et al. (2012a)). While homeostasis  
442 also includes storage and remobilization of a controlled variable (Huang et al.  
443 (2012)), we have for the sake of simplicity omitted the vacuolar storage of  
444 sucrose and its remobilization from the store (Endler et al. (2006)).

445  
446 The negative feedback loop containing  $E_{in,0}^{sucrose}$  (Fig. 1) is described as  
447 an inflow controller motif, which keeps sucrose at a constant level when  
448 the demand for sucrose is high, i.e., when sufficient resources are available,  
449 the plant is growing and the primary C-flux is high. A molecular compo-  
450 nent involved in an inflow negative feedback regulation of sucrose is SnRK1  
451 (Sucrose non-fermenting -1- Related protein Kinase), which is activated by  
452 sucrose (Tognetti et al. (2013)). SnRK1 on its side inactivates Sucrose 6F-  
453 phosphatase, an enzyme involved in the synthesis of sucrose. Thus, SnRK1  
454 and sucrose are linked by a negative feedback loop that has an inflow control  
455 structure with respect to sucrose (motif 2, Drengstig et al. (2012a)). Another  
456 important factor which is related in the control of the primary C-flux and  
457 plant growth is the kinase TARGET OF RAPAMYCIN (TOR) (Menand  
458 et al. (2002)). Growth stops when TOR is silenced in Arabidopsis plants by  
459 using different RNA interference strategies (Deprost et al. (2007); Dobrenel  
460 et al. (2011); Caldana et al. (2013)). While these studies indicate that TOR  
461 is involved in plant growth and in the regulation of the primary C-flux, the  
462 feedback mechanisms from the primary C-compounds regulating TOR are  
463 presently not well understood.

464  
465 The negative feedback including  $E_{out,fl}^{phe}$  and responsible for the induction  
466 of the secondary C-flux, i.e., the upregulation of phenolics under low N con-  
467 ditions, is described as an outflow controller, which moves the accumulating  
468 sucrose (due to the decreased primary C-flux at these conditions) into the  
469 secondary metabolism. The feedback loop is based on a sucrose-specific in-  
470 duction of PAP1 (Teng et al. (2005); Solfanelli et al. (2006)). PAP1 induces  
471 TT8, which together with TTG1 and PAP1 activate the phenolic pathway  
472 (Baudry et al. (2006); Dubos et al. (2008); Matsui et al. (2008)), and thereby  
473 consumes sucrose. Interestingly, this sucrose regulating feedback loop con-  
474 tains a positive and a negative feedback loop both regulating the global  
475 transcription factors PAP1, TT8 and others (Baudry et al. (2006); Dubos  
476 et al. (2008); Matsui et al. (2008)). TT8 has been found to be produced in a  
477 self-amplifying (autocatalytic) manner (Baudry et al. (2006)) and associating  
478 in the ternary complex MBW, which includes TT8 and TTG1. MBW acti-

479 vates the synthesis of anthocyanins. Fig. 8a shows a possible scenario of the  
480 negative feedback regulation. The autocatalytic formation of TT8 combined  
481 with a first-order removal of TT8 provides an effective control (Drengstig  
482 et al. (2012b)) of PAP1, while the activation of the anthocyanin synthesis  
483 by MBW closes the negative feedback regulation of sucrose. The set-point  
484 of sucrose for this outflow controller is determined by the rate equation for  
485 PAP1. In case  $k_{65}$  (which is considered as the Michaelis constant for the  
486 PAP1-removing/inactivating enzyme) is low compared to the concentration  
487 of PAP1, the sucrose set-point is given by the ratio  $k_{64}/k_{63}$  (Drengstig et al.  
488 (2012a)). The set-point for PAP1 is determined by the rate equation for TT8  
489 and given as the ratio  $k_{67}/k_{66}$ . Fig. 8b shows the behavior of the system when  
490 the steady state is perturbed by a sudden increase of sucrose at  $t=50$  time  
491 units. The adaptation of sucrose and PAP1 to their respective set-points is  
492 clearly seen and is in qualitative agreement with experimental results (Figs.6a  
493 and 6b in Solfanelli et al. (2006)). Fig. 8c shows a comparison of the system's  
494 response behavior with and without an autocatalytic production in TT8. To  
495 keep PAP1 still under a homeostatic regulation, rate constant  $k_{70}$  (which  
496 corresponds to the Michaelis constant of a TT8-removing/inactivating en-  
497 zyme) has been added. When  $k_{70} \ll \text{TT8}$  the set-point for PAP1 is the same  
498 as in the autocatalytic case, i.e.  $PAP1_{set} = k_{67}/k_{66}$ . The response time of the  
499 system when TT8 is formed autocatalytically is considerably shorter, while  
500 no practical differences in the MBW and TT8 kinetics were observed. The  
501 increased effectiveness of PAP1 regulation by autocatalysis may be a reason  
502 why a control structure with a positive feedback has developed.

503

504 The transcription factor MYBL2 has been identified as a negative regu-  
505 lator of the anthocyanin biosynthesis pathway (Dubos et al. (2008); Matsui  
506 et al. (2008)). High external sucrose levels down-regulate MYBL2 signifi-  
507 cantly, while under normal growing conditions the transcript levels of MYBL2  
508 appear unaffected (Nemie-Feyissa et al. (2014)). To what extent MYBL2 par-  
509 ticipates in the switch to secondary metabolism/antocyanins when N levels  
510 are low is presently not known and we have therefore not included MYBL2  
511 in the model.

512

513 N has been found to be a global regulator of a variety of processes includ-  
514 ing activation of photosynthesis, chlorophyll production, primary metabo-  
515 lites (Scheible et al. (2004)) and repression of starch metabolism (Scheible  
516 et al. (1997)). On the other hand, N inhibits the synthesis of phenylalanine

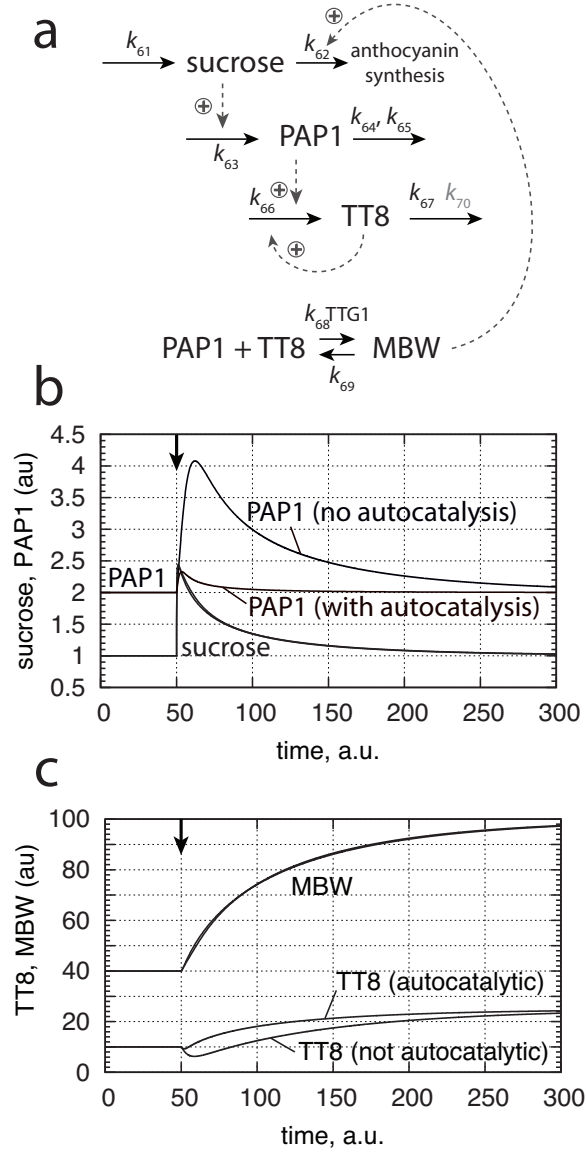


Figure 8: Comparison of autocatalytic and non-autocatalytic regulation of PAP1 and sucrose. (a) Reaction mechanism. For rate equations see Appendix. (b) At time  $t=50$  (arrow)  $k_{61}$  is increased from 4.0 to 10.0. PAP1 is regulated more rapidly by the autocatalytic mechanism. Set-points for sucrose and PAP1 are 1.0 and 2.0, respectively. (c) Behavior of the controller molecules MBW and TT8. Rate constants:  $k_{62}=0.1, k_{63}=k_{64}=1.0, k_{65}=1.0 \times 10^{-4}, k_{66}=0.5, k_{67}=1.0, k_{68}^{TTG1}=2.0, k_{69}=1.0, k_{70}=1.0 \times 10^{-4}$ . Initial concentrations:  $\text{sucr}_0=1.0, \text{PAP1}_0=2.0, \text{TT8}_0=10.0, \text{MBW}_0=40.0$ .



517 (Scheible et al. (2004)) as well as the production of anthocyanins by inhibit-  
518 ing the production/activities of PAP1 and PAP2 using the LBD-family of  
519 transcription factors (Rubin et al. (2009)). These various activation and inhi-  
520 bition processes by N are described in the model by the respective activating  
521 and inhibition functions  $f_{act}$  and  $f_I$  originating from internal N (Fig. 1). N  
522 is also a signal contributing to transcriptional regulation of genes coding for  
523 key enzymes of the phenylpropanoid pathway (PAL, C4H, 4CL; Fritz et al.  
524 (2006)).

525

526 The typical saw-tooth behavior of starch build-up and consumption is  
527 well reflected by the model. During the day, triose-phosphate levels are kept  
528 approximately constant such that the rate of starch synthesis under light con-  
529 ditions is approximately constant. During the night, the  $E_{infl}^{starch}$  controller  
530 maintains sucrose homeostasis and compensates for the (constant) rate of  
531 total sucrose consumption by primary and secondary C-fluxes. In this re-  
532 spect, the constant synthesis and degradation rates for starch in the model  
533 are closely related to the regulation of triose-phosphate and sucrose home-  
534 ostasis.

535

536 Thus, sucrose homeostasis, regulation of starch content and its adaptation  
537 to light-dark regimes, and the diversion of primary C-flux into secondary  
538 metabolism are integrated and interconnected mechanisms. The fine-tuned  
539 regulation of the allocation of C to secondary metabolism plays a prominent  
540 role in plant defense responses under abiotic and biotic constraints and allows  
541 to optimize costs of defense.

## 542 7. Acknowledgment

543 This work was supported in part by a Marie Curie exchange program  
544 between the University of Lorraine, France, and the University of Stavanger,  
545 Norway and by INRA "Département Environnement et Agronomie" through  
546 a grant allowed to P.R.

## 547 Appendix A. Rate Equations of Model

548 Grayed sections in Fig. 1 are added in the calculations of Fig. 7. Abbre-  
549 viations: N, internal nitrate;  $N_{ext}$ , external nitrate; trioseP, triose phosphate;  
550 sucr, sucrose.

$$\begin{aligned} \frac{d \text{sucr}}{dt} &= k_4 \cdot E_{infl}^{trioseP} \cdot \text{trioseP} - k_9 \cdot \text{sucr} \cdot E_{outfl}^{phe} \cdot f_I^{phe} - k_5 \cdot \text{sucr} \cdot f_{act}^{pcf} \\ &\quad - (k_{14} + k_{15}) \cdot \text{sucr} + k_{37} \cdot \text{starch} \cdot E_{infl}^{starch}; \quad f_I^{phe} = \frac{k_{38}}{k_{38} + N}; \quad f_{act}^{pcf} = \frac{N}{k_{13} + N} \end{aligned} \quad (\text{A.1})$$

$$\frac{d E_{infl}^{trioseP}}{dt} = k_1 - \frac{k_2 \cdot \text{sucr} \cdot E_{infl}^{trioseP}}{k_3 + E_{infl}^{trioseP}} \quad (\text{A.2})$$

$$\frac{d E_{outfl}^{phe}}{dt} = k_6 \cdot \text{sucr} \cdot f_I^{E_{outfl}^{phe}} - \frac{k_7 \cdot E_{outfl}^{phe}}{k_8 + E_{outfl}^{phe}}; \quad f_I^{E_{outfl}^{phe}} = \frac{k_{39}}{k_{39} + N} \quad (\text{A.3})$$

$$\frac{d N}{dt} = k_{11} \cdot N_{ext} \cdot E_{infl}^{nitrate} - k_{12} \cdot N \quad (\text{A.4})$$

$$\frac{d N_{ext}}{dt} = -g \cdot k_{11} \cdot N_{ext} \cdot E_{infl}^{nitrate} \quad (\text{A.5})$$

551  $g$ : scaling factor due to the size of the external volume

552

553

$$\frac{d \text{starch}}{dt} = k_{10} \cdot \text{trioseP} - k_{37} \cdot \text{starch} \cdot E_{infl}^{starch} \quad (\text{A.6})$$

$$\frac{d E_{infl}^{nitrate}}{dt} = k_{26} - \frac{k_{27} \cdot N \cdot E_{infl}^{nitrate}}{k_{28} + E_{infl}^{nitrate}} \quad (\text{A.7})$$

$$\frac{d \text{trioseP}}{dt} = k_{29} \cdot f_{act}^{trioseP} \cdot E_{infl}^{CO_2} - (k_4 \cdot E_{infl}^{trioseP} + k_{10}) \cdot \text{trioseP} \quad (\text{A.8})$$

$$554 \quad f_{act}^{trioseP} = \frac{N}{k_{33} + N}$$

555

556

$$\frac{d E_{infl}^{CO_2}}{dt} = k_{30} - \frac{k_{31} \cdot \text{trioseP} \cdot E_{infl}^{CO_2}}{k_{32} + E_{infl}^{CO_2}} \quad (\text{A.9})$$

$$\frac{d E_{infl}^{starch}}{dt} = k_{34} - \frac{k_{35} \cdot \text{sucr} \cdot E_{infl}^{starch}}{k_{36} + E_{infl}^{starch}} \quad (\text{A.10})$$

557 When the adaptation to minimum starch levels at different LD regimes  
 558 using MM kinetics is included (grayed sections in Fig. 1; results given in  
 559 Fig. 7) the rate equations for triose-phosphate, starch, and  $E_{infl}^{TP}$  change to:

$$\frac{d starch}{dt} = \frac{k_{10} \cdot trioseP \cdot f_I}{k_{49} + trioseP} - k_{37} \cdot starch \cdot E_{infl}^{starch} \quad (A.11)$$

560 with  $f_I = \frac{k_{56}}{k_{56} + E_{infl}^{TP}}$   
 561

$$\frac{d trioseP}{dt} = k_{29} \cdot f_{act}^{trioseP} \cdot E_{infl}^{CO_2} - \left( k_4 \cdot E_{infl}^{trioseP} + \frac{f_I \cdot k_{10}}{k_{49} + trioseP} \right) \cdot trioseP \quad (A.12)$$

562  $f_{act}^{trioseP}$  and  $f_I$  are as described under Eq. A.8 and Eq. A.11, respectively.

$$\frac{d E_{infl}^{TP}}{dt} = k_{53} \cdot starch - \frac{k_{54} \cdot E_{infl}^{TP}}{k_{55} + E_{infl}^{TP}} \quad (A.13)$$

563

564

565 **Appendix B. Rate Equations for Daylength Measuring Mechanism**  
 566 **in Fig. 6a**

$$\frac{d M1}{dt} = k_{29} \cdot k_{40} - \frac{k_{44} \cdot K_I^L \cdot M1}{K_I^L + k_{29}} \quad (B.1)$$

$$\frac{d M2}{dt} = \frac{k_{44} \cdot K_I^L \cdot M1}{K_I^L + k_{29}} - \frac{k_{29} \cdot k_{40} \cdot M2}{K_M^{M2} + M2} \quad (B.2)$$

567

568

569 **Appendix C. Rate Equations for Daylength Measuring Mechanism**  
 570 **in Fig. 6d**

$$\frac{d M}{dt} = k_{50} - k_{51} \cdot M \cdot E; \text{ with } k_{50} = f_{act}^M = \frac{k_{29}}{K_a^L + k_{29}} \quad (C.1)$$

$$\frac{dE}{dt} = k_{52} \cdot M - \frac{k_{53} \cdot E}{K_M^E + E} \quad (\text{C.2})$$

571

572

573 **Appendix D. Rate Equations for Sucrose and PAP1 Regulation by**  
 574 **TT8/MBW (Fig. 8a)**

$$\frac{d \textit{sucr}}{dt} = k_{61} - k_{62} \cdot \textit{sucr} \cdot \textit{MBW} \quad (\text{D.1})$$

$$\frac{d \textit{PAP1}}{dt} = k_{63} \cdot \textit{sucr} - \frac{k_{64} \textit{PAP1}}{k_{65} + \textit{PAP1}} - k_{68}^{\textit{TTG1}} \cdot \textit{PAP1} \cdot \textit{TT8} + k_{69} \cdot \textit{MBW} \quad (\text{D.2})$$

$$\frac{d \textit{MBW}}{dt} = k_{68}^{\textit{TTG1}} \cdot \textit{PAP1} \cdot \textit{TT8} - k_{69} \cdot \textit{MBW} \quad (\text{D.3})$$

575

576 **Non-autocatalytic regulation of PAP1:**

$$\frac{d \textit{TT8}}{dt} = k_{66} \cdot \textit{PAP1} - \frac{k_{67} \cdot \textit{TT8}}{k_{70} + \textit{TT8}} - k_{68}^{\textit{TTG1}} \cdot \textit{PAP1} \cdot \textit{TT8} + k_{69} \cdot \textit{MBW} \quad (\text{D.4})$$

577

578 **Autocatalytic regulation of PAP1:**

$$\frac{d \textit{TT8}}{dt} = k_{66} \cdot \textit{PAP1} \cdot \textit{TT8} - k_{67} \cdot \textit{TT8} - k_{68}^{\textit{TTG1}} \cdot \textit{PAP1} \cdot \textit{TT8} + k_{69} \cdot \textit{MBW} \quad (\text{D.5})$$

579

580

581 Abro, M. A., Lecompte, F., Bryone, F., Nicot, P. C., 2013. Nitrogen fertiliza-  
 582 tion of the host plant influences production and pathogenicity of botrytis  
 583 cinerea secondary inoculum. *Phytopathology* 103 (3), 261–267.

584 Baudry, A., Caboche, M., Lepiniec, L., 2006. TT8 controls its own expression  
 585 in a feedback regulation involving TTG1 and homologous MYB and bHLH  
 586 factors, allowing a strong and cell-specific accumulation of flavonoids in  
 587 *Arabidopsis thaliana*. *The Plant Journal* 46 (5), 768–779.

- 588 Bryant, J. P., Chapin III, F. S., Klein, D. R., 1983. Carbon/nutrient balance  
589 of boreal plants in relation to vertebrate herbivory. *Oikos*, 357–368.
- 590 Bünning, E., 1973. *The Physiological Clock. Circadian Rhythms and Biolog-*  
591 *ical Chronometry.* Springer-Verlag, Berlin.
- 592 Caldana, C., Li, Y., Leisse, A., Zhang, Y., Bartholomaeus, L., Fernie, A. R.,  
593 Willmitzer, L., Giavalisco, P., 2013. Systemic analysis of inducible target  
594 of rapamycin mutants reveal a general metabolic switch controlling growth  
595 in *arabidopsis thaliana*. *The Plant Journal* 73 (6), 897–909.
- 596 Cannon, W., 1929. Organization for Physiological Homeostasis. *Physiol. Rev.*  
597 9, 399–431.
- 598 Deprost, D., Yao, L., Sormani, R., Moreau, M., Leterreux, G., Nicolai, M.,  
599 Bedu, M., Robaglia, C., Meyer, C., 2007. The Arabidopsis TOR kinase  
600 links plant growth, yield, stress resistance and mRNA translation. *EMBO*  
601 *Reports* 8 (9), 864–870.
- 602 Dijkwel, P. P., Kock, P. A., Bezemer, R., Weisbeek, P. J., Smeeckens, S. C.,  
603 1996. Sucrose represses the developmentally controlled transient activation  
604 of the plastocyanin gene in *Arabidopsis thaliana* seedlings. *Plant Physiol-*  
605 *ogy* 110 (2), 455–463.
- 606 Dobrenel, T., Marchive, C., Sormani, R., Moreau, M., Mozzo, M., Montané,  
607 M.-H., Menand, B., Robaglia, C., Meyer, C., 2011. Regulation of plant  
608 growth and metabolism by the TOR kinase. *Biochemical Society Transac-*  
609 *tions* 39 (2), 477–481.
- 610 Doré, T., Makowski, D., Malézieux, E., Munier-Jolain, N., Tchamitchian,  
611 M., Tittone, P., 2011. Facing up to the paradigm of ecological intensifica-  
612 tion in agronomy: revisiting methods, concepts and knowledge. *European*  
613 *Journal of Agronomy* 34 (4), 197–210.
- 614 Drengstig, T., Jolma, I., Ni, X., Thorsen, K., Xu, X., Ruoff, P., 2012a. A  
615 basic set of homeostatic controller motifs. *Biophys J* 103 (9), 2000–2010.
- 616 Drengstig, T., Ni, X., Thorsen, K., Jolma, I., Ruoff, P., 2012b. Robust adap-  
617 tation and homeostasis by autocatalysis. *The Journal of Physical Chem-*  
618 *istry B* 116 (18), 5355–5363.

- 619 Dubos, C., Le Gourrierc, J., Baudry, A., Huep, G., Lanet, E., Debeaujon, I.,  
620 Routaboul, J.-M., Alboresi, A., Weisshaar, B., Lepiniec, L., 2008. MYBL2  
621 is a new regulator of flavonoid biosynthesis in *Arabidopsis thaliana*. The  
622 Plant Journal 55 (6), 940–953.
- 623 Eimert, K., Wang, S.-M., Lue, W., Chen, J., 1995. Monogenic recessive  
624 mutations causing both late floral initiation and excess starch accumulation  
625 in Arabidopsis. The Plant Cell 7 (10), 1703–1712.
- 626 Endler, A., Meyer, S., Schelbert, S., Schneider, T., Weschke, W., Peters,  
627 S. W., Keller, F., Baginsky, S., Martinoia, E., Schmidt, U. G., 2006. Iden-  
628 tification of a vacuolar sucrose transporter in barley and Arabidopsis mes-  
629 ophyll cells by a tonoplast proteomic approach. Plant Physiology 141 (1),  
630 196–207.
- 631 Farquhar, G., von Caemmerer, S. v., Berry, J., 1980. A biochemical model  
632 of photosynthetic CO<sub>2</sub> assimilation in leaves of C<sub>3</sub> species. Planta 149 (1),  
633 78–90.
- 634 Feugier, F. G., Satake, A., 2013. Dynamical feedback between cir-  
635 cadian clock and sucrose availability explains adaptive response of  
636 starch metabolism to various photoperiods. Front. Plant Sci 3 (305),  
637 doi: 10.3389/fpls.2012.00305.
- 638 Fritz, C., Palacios-Rojas, N., Feil, R., Stitt, M., 2006. Regulation of sec-  
639 ondary metabolism by the carbon–nitrogen status in tobacco: nitrate in-  
640 hibits large sectors of phenylpropanoid metabolism. The Plant Journal  
641 46 (4), 533–548.
- 642 Garner, W. W., Allard, H. A., 1920. Effect of the relative length of day and  
643 night and other factors of the environment on growth and reproduction in  
644 plants. Journal of Agricultural Research (Washington, D.C.) 18, 553–606.
- 645 Geiger, M., Haake, V., Ludewig, F., Sonnewald, U., Stitt, M., 1999. The ni-  
646 trate and ammonium nitrate supply have a major influence on the response  
647 of photosynthesis, carbon metabolism, nitrogen metabolism and growth to  
648 elevated carbon dioxide in tobacco. Plant, Cell & Environment 22 (10),  
649 1177–1199.
- 650 Gibon, Y., Bläsing, O. E., Palacios-Rojas, N., Pankovic, D., Hendriks, J. H.,  
651 Fisahn, J., Höhne, M., Günther, M., Stitt, M., 2004. Adjustment of diurnal

- 652 starch turnover to short days: depletion of sugar during the night leads to  
653 a temporary inhibition of carbohydrate utilization, accumulation of sugars  
654 and post-translational activation of ADP-glucose pyrophosphorylase in the  
655 following light period. *The Plant Journal* 39 (6), 847–862.
- 656 Glynn, C., Herms, D. A., Orians, C. M., Hansen, R. C., Larsson, S., 2007.  
657 Testing the growth–differentiation balance hypothesis: dynamic responses  
658 of willows to nutrient availability. *New Phytologist* 176 (3), 623–634.
- 659 Hanson, J., Hanssen, M., Wiese, A., Hendriks, M. M., Smeekens, S.,  
660 2008. The sucrose regulated transcription factor bZIP11 affects amino  
661 acid metabolism by regulating the expression of ASPARAGINE SYN-  
662 THETASE1 and PROLINE DEHYDROGENASE2. *The Plant Journal*  
663 53 (6), 935–949.
- 664 Herms, D. A., Mattson, W. J., 1992. The Dilemma of Plants: To Grow or  
665 Defend. *Quarterly Review of Biology* 67 (3), 283–335.
- 666 Huang, Y., Drensting, T., Ruoff, P., 2012. Integrating fluctuating nitrate up-  
667 take and assimilation to robust homeostasis. *Plant, Cell and Environment*  
668 35, 917–928.
- 669 Huber, S., Huber, J., McMichael, R., 1992. The Regulation of Sucrose Syn-  
670 thesis in Leaves. In: Pollock, C., Farrar, J., Gordon, A. (Eds.), *Carbon*  
671 *Partitioning: Within and Between Organisms*. Bios Scientific Publishers,  
672 Oxford,, pp. 1–26.
- 673 Kallarackal, J., Bauer, S. N., Nowak, H., Hajirezaei, M.-R., Komor, E., 2012.  
674 Diurnal changes in assimilate concentrations and fluxes in the phloem of  
675 castor bean (*Ricinus communis* L.) and tansy (*Tanacetum vulgare* L.).  
676 *Planta* 236 (1), 209–223.
- 677 Kingston-Smith, A. H., Bollard, A. L., Minchin, F. R., 2005. Stress-induced  
678 changes in protease composition are determined by nitrogen supply in non-  
679 nodulating white clover. *Journal of Experimental Botany* 56 (412), 745–  
680 753.
- 681 Koricheva, J., Larsson, S., Haukioja, E., Keinänen, M., 1998. Regulation  
682 of woody plant secondary metabolism by resource availability: hypothesis  
683 testing by means of meta-analysis. *Oikos*, 212–226.

- 684 Larbat, R., Le Bot, J., Bourgaud, F., Robin, C., Adamowicz, S., 2012. Organ-  
685 specific responses of tomato growth and phenolic metabolism to nitrate  
686 limitation. *Plant Biology* 14 (5), 760–769.
- 687 Le Bot, J., Bénard, C., Robin, C., Bourgaud, F., Adamowicz, S., 2009. The  
688 trade-off between synthesis of primary and secondary compounds in young  
689 tomato leaves is altered by nitrate nutrition: experimental evidence and  
690 model consistency. *Journal of Experimental Botany* 60, 4301–4314.
- 691 Lillo, C., Lea, U. S., Ruoff, P., 2008. Nutrient depletion as a key factor for  
692 manipulating gene expression and product formation in different branches  
693 of the flavonoid pathway. *Plant, Cell & Environment* 31 (5), 587–601.
- 694 Loomis, W., 1932. Growth-differentiation balance vs. carbohydrate-nitrogen  
695 ratio. *Proc. Am. Soc. Hortic. Sci.* 29, 240–245.
- 696 Lu, Y., Gehan, J. P., Sharkey, T. D., 2005. Daylength and circadian effects  
697 on starch degradation and maltose metabolism. *Plant Physiology* 138 (4),  
698 2280–2291.
- 699 Marschner, P., 2012. *Marschner's Mineral Nutrition of Higher Plants*. Third  
700 Edition. Academic Press.
- 701 Massad, T. J., Dyer, L. A., Vega, G., 2012. Costs of defense and a test of the  
702 carbon-nutrient balance and growth-differentiation balance hypotheses for  
703 two co-occurring classes of plant defense. *PLOS ONE* 7 (10), e47554.
- 704 Matsui, K., Umemura, Y., Ohme-Takagi, M., 2008. *Atmyb12*, a protein with a  
705 single myb domain, acts as a negative regulator of anthocyanin biosynthesis  
706 in arabidopsis. *The Plant Journal* 55 (6), 954–967.
- 707 McKey, D., 1974. Adaptive patterns in alkaloid physiology. *American Natu-*  
708 *ralist*, 305–320.
- 709 Menand, B., Desnos, T., Nussaume, L., Berger, F., Bouchez, D., Meyer, C.,  
710 Robaglia, C., 2002. Expression and disruption of the Arabidopsis TOR  
711 (Target Of Rapamycin) gene. *PNAS* 99 (9), 6422–6427.
- 712 Miller, A. J., Smith, S. J., 1992. The mechanism of nitrate transport across  
713 the tonoplast of barley root cells. *Planta* 187 (4), 554–557.



- 714 Miller, A. J., Smith, S. J., 2008. Cytosolic nitrate ion homeostasis: could it  
715 have a role in sensing nitrogen status? *Annals of Botany* 101 (4), 485–489.
- 716 Mooney, K. A., Halitschke, R., Kessler, A., Agrawal, A. A., 2010. Evolution-  
717 ary trade-offs in plants mediate the strength of trophic cascades. *Science*  
718 327 (5973), 1642–1644.
- 719 Nemie-Feyissa, D., Olafsdottir, S. M., Heidari, B., Lillo, C., 2014. Nitrogen  
720 depletion and small R3-MYB transcription factors affecting anthocyanin  
721 accumulation in *Arabidopsis* leaves. *Phytochemistry* 98, 34–40.
- 722 Nguyen, P. M., Niemeyer, E. D., 2008. Effects of nitrogen fertilization on  
723 the phenolic composition and antioxidant properties of basil (*Ocimum*  
724 *basilicum* L.). *Journal of Agricultural and Food Chemistry* 56 (18), 8685–  
725 8691.
- 726 Ni, X., Drengstig, T., Ruoff, P., 2009. The control of the controller: Molecular  
727 mechanisms for robust perfect adaptation and temperature compensation.  
728 *Biophys J* 97, 1244–53.
- 729 Peuke, A., Rokitta, M., Zimmermann, U., Schreiber, L., Haase, A., 2001.  
730 Simultaneous measurement of water flow velocity and solute transport in  
731 xylem and phloem of adult plants of *Ricinus communis* over a daily time  
732 course by Nuclear Magnetic Resonance Spectrometry. *Plant, Cell & Envi-*  
733 *ronment* 24 (5), 491–503.
- 734 Pokhilko, A., Ebenhöf, O., 2015. Mathematical modelling of diurnal regula-  
735 tion of carbohydrate allocation by osmo-related processes in plants. *Journal*  
736 *of The Royal Society Interface* 12 (104), 20141357.
- 737 Pokhilko, A., Flis, A., Sulpice, R., Stitt, M., Ebenhöf, O., 2014. Adjustment  
738 of carbon fluxes to light conditions regulates the daily turnover of starch  
739 in plants: a computational model. *Molecular BioSystems* 10 (3), 613–627.
- 740 Pretorius, J., Nieuwoudt, D., Eksteen, D., 1999. Sucrose synthesis and  
741 translocation in *Zea mays* L. during early growth, when subjected to N  
742 and K deficiency. *South African Journal of Plant and Soil* 16 (4), 173–179.
- 743 Radhakrishnan, K., Hindmarsh, A., 1993. Description and Use of LSODE,  
744 the Livermore Solver for Ordinary Differential Equations. NASA Refer-  
745 ence Publication 1327, Lawrence Livermore National Laboratory Report

- 746 UCRL-ID-113855. National Aeronautics and Space Administration, Lewis  
747 Research Center, Cleveland, OH 44135-3191.
- 748 Romberger, J. A., 1963. Meristems, growth, and development in woody  
749 plants: An analytical review of anatomical, physiological, and morphogenic  
750 aspects. No. 1293. US Government Printing Office.
- 751 Royer, M., Larbat, R., Le Bot, J., Adamowicz, S., Robin, C., 2013. Is the C:  
752 N ratio a reliable indicator of C allocation to primary and defence-related  
753 metabolisms in tomato? *Phytochemistry* 88, 25–33.
- 754 Rubin, G., Tohge, T., Matsuda, F., Saito, K., Scheible, W.-R., 2009. Mem-  
755 bers of the LBD family of transcription factors repress anthocyanin syn-  
756 thesis and affect additional nitrogen responses in Arabidopsis. *The Plant*  
757 *Cell* 21 (11), 3567–3584.
- 758 Scheible, W.-R., Lauerer, M., Schulze, E.-D., Caboche, M., Stitt, M., 1997.  
759 Accumulation of nitrate in the shoot acts as a signal to regulate shoot-root  
760 allocation in tobacco. *The Plant Journal* 11 (4), 671–691.
- 761 Scheible, W.-R., Morcuende, R., Czechowski, T., Fritz, C., Osuna, D.,  
762 Palacios-Rojas, N., Schindelasch, D., Thimm, O., Udvardi, M. K.,  
763 Stitt, M., 2004. Genome-wide reprogramming of primary and secondary  
764 metabolism, protein synthesis, cellular growth processes, and the regula-  
765 tory infrastructure of Arabidopsis in response to nitrogen. *Plant Physiology*  
766 136 (1), 2483–2499.
- 767 Scialdone, A., Howard, M., 2015. How plants manage food reserves at night:  
768 quantitative models and open questions. *Frontiers in Plant Science* 6, 204.
- 769 Scialdone, A., Mugford, S. T., Feike, D., Skeffington, A., Borrill, P., Graf, A.,  
770 Smith, A. M., Howard, M., 2013. Arabidopsis plants perform arithmetic  
771 division to prevent starvation at night. *Elife* 2, e00669.
- 772 Seaton, D. D., Ebenhöf, O., Millar, A. J., Pokhilko, A., 2014. Regulatory  
773 principles and experimental approaches to the circadian control of starch  
774 turnover. *Journal of The Royal Society Interface* 11 (91), 20130979.
- 775 Smith, A. M., Stitt, M., 2007. Coordination of carbon supply and plant  
776 growth. *Plant, Cell & Environment* 30 (9), 1126–1149.

- 777 Smith, J. A. C., Milburn, J. A., 1980. Phloem transport, solute flux and the  
778 kinetics of sap exudation in *Ricinus communis* L. *Planta* 148 (1), 35–41.
- 779 Solfanelli, C., Poggi, A., Loreti, E., Alpi, A., Perata, P., 2006. Sucrose-specific  
780 induction of the anthocyanin biosynthetic pathway in *Arabidopsis*. *Plant*  
781 *Physiology* 140 (2), 637–646.
- 782 Stamp, N., 2003. Out of the quagmire of plant defense hypotheses. *The Quar-*  
783 *terly Review of Biology* 78 (1), 23–55.
- 784 Stamp, N., 2004. Can the growth–differentiation balance hypothesis be tested  
785 rigorously? *Oikos* 107 (2), 439–448.
- 786 Stewart, A., Chapman, W., Jenkins, G., Graham, I., Martin, T., Crozier,  
787 A., 2001. The effect of nitrogen and phosphorus deficiency on flavonol  
788 accumulation in plant tissues. *Plant, Cell & Environment* 24 (11), 1189–  
789 1197.
- 790 Stitt, M., Zeeman, S. C., 2012. Starch turnover: pathways, regulation and  
791 role in growth. *Current Opinion in Plant Biology* 15 (3), 282–292.
- 792 Taiz, L., Zeiger, E., Møller, I. M., Murphy, A. S., 2015. *Plant Physiology and*  
793 *Development*. Sinauer, Sunderland.
- 794 Teng, S., Keurentjes, J., Bentsink, L., Koornneef, M., Smeekeens, S., 2005.  
795 Sucrose-specific induction of anthocyanin biosynthesis in *Arabidopsis* re-  
796 quires the MYB75/PAP1 gene. *Plant Physiology* 139 (4), 1840–1852.
- 797 Thorsen, K., Drengstig, T., Ruoff, P., 2013. Control Theoretic Properties  
798 of Physiological Controller Motifs. In: *ICSSE 2013, IEEE International*  
799 *Conference on System Science and Engineering*. Budapest, pp. 165–170.
- 800 Tognetti, J. A., Horacio, P., Martinez-Noel, G., 2013. Sucrose signaling in  
801 plants: A world yet to be explored. *Plant Signaling & Behavior* 8 (3),  
802 e23316.
- 803 Vidal, E. A., Gutierrez, R. A., 2008. A systems view of nitrogen nutrient and  
804 metabolite responses in *Arabidopsis*. *Current Opinion in Plant Biology*  
805 11 (5), 521–529.

- 806 Von Caemmerer, S. v., Farquhar, G., 1981. Some relationships between the  
807 biochemistry of photosynthesis and the gas exchange of leaves. *Planta*  
808 153 (4), 376–387.
- 809 Wilkie, J., Johnson, M., Reza, K., 2002. *Control Engineering. An Introductory*  
810 *Course*. Palgrave, New York.
- 811 Wind, J., Smeeckens, S., Hanson, J., 2010. Sucrose: metabolite and signaling  
812 molecule. *Phytochemistry* 71 (14), 1610–1614.
- 813 Xu, G., Fan, X., Miller, A. J., 2012. Plant nitrogen assimilation and use  
814 efficiency. *Annual Review of Plant Biology* 63, 153–182.
- 815 Yi, T., Huang, Y., Simon, M., Doyle, J., 2000. Robust perfect adaptation  
816 in bacterial chemotaxis through integral feedback control. *PNAS* 97 (9),  
817 4649–53.
- 818 Zhang, X., Myers, A. M., James, M. G., 2005. Mutations affecting starch  
819 synthase iii in arabidopsis alter leaf starch structure and increase the rate  
820 of starch synthesis. *Plant Physiology* 138 (2), 663–674.
- 821 Züst, T., Joseph, B., Shimizu, K. K., Kliebenstein, D. J., Turnbull, L. A.,  
822 2011. Using knockout mutants to reveal the growth costs of defensive  
823 traits. *Proceedings of the Royal Society of London B: Biological Sciences*,  
824 doi:10.1098/rspb.2010.2475.